# EXPERIMENTAL RESULTS OF BEAM HALO AT IHEP *

H.F. Ouyang#, J. Peng, T. Huang, J. Li, T.G. Xu, IHEP, CAS, Beijing 100049, China

*Abstract*

Space-charge forces acting in mismatched beams have been identified as a major cause of beam halo. In this paper, we describe the beam halo experimental results in a FODO beam line at IHEP. With this beam transport line, experiments are firstly carried out to determine the main beam parameters at the exit of a RFQ with intense beams, and then the measured beam profiles at different positions are compared with the multi-particle simulation profiles to study the formation of beam halo. The maximum measured amplitudes of the matched and mismatched beam profiles agreed well with simulations. Details of the experiment will be presented.

## INTRODUCTION

High-power and high-intensity proton beams are becoming more and more widely applied in the related fields such as neutron spallation source, accelerator driven sub-critical system (ADS) for transmutation of nuclear waste, etc. One of the important characteristics of high-intensity beams is the existence of halo and its hard unavoidability. Because the halo particles tend to be lost easily on the walls of the beam line structures and induce unwanted radioactivity, the interest in understanding the beam halo formation has increased.

Space-charge forces acting in mismatched beams have been commonly identified as a major cause of beam halo. It is found that the mismatch can produce coherent oscillations of the RMS beam size. Individual beam particles interact with the time-varying space charge field due to the beam density oscillation in the beam core, acquire enough transverse energy and then become parts of the halo [1]. In order to understand this process, large numbers of theoretical literature [2] have evolved and large numbers of computer simulations have been carried out [3]. However, few beam experiments have been done, owing in part to the fact that few intense proton beams with the required intensity exist [4]. Fortunately, by making use of the available intense proton beams from a radio frequency quadrupole (RFQ) accelerator designated for ADS study at the Institute of High Energy Physics (IHEP), we have set up a 28-quadrupole beam transport line as the platform to study the beam halo experimentally. It is the first domestic beam line dedicated for the halo study of high intensity proton beam.

## THE BEAM HALO EXPERIMENT TRANSPORT LINE

The 28-quadrupole beam transport line is installed after a 325MHz RFQ with intense beams. The output energy and the design beam current for this RFQ are 3.5MeV and 50mA, respectively. The purpose of this transport line is the experimental study of the beam halo formation. The schematic layout of this transport line is shown in Fig. 1. In this line, the first four quadruples are used to establish match or mismatch conditions for the halo formation, the last 24 quadruples are used to constitute a period FODO lattice. The quadrupole magnets are spaced 19cm each other so that the beam diagnostic devices can be mounted between them. In Table 1, the quadrupole magnet length, gradient and the beam pipe diameter are given. The matched RMS beam radius foreseen is about 0.15cm, while the beam pipe diameter is designed to 3.6cm, which is more than 10 times the RMS beam size.

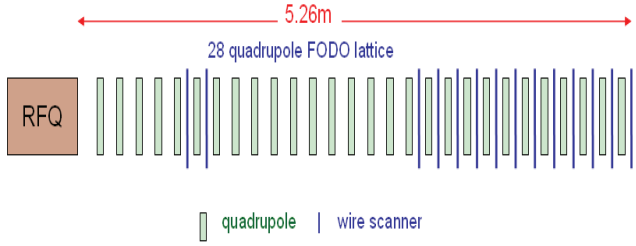


Figure 1: Layout of the beam halo experiment transport line.

Table 1: Parameters of the Experiment Transport Line

| Q magnet number | 1 | 2 | 3 | 4 | 5-28 |
|---|---|---|---|---|---|
| Max gradient (T/m) | 30 | 30 | 30 | 30 | 30 |
| Magnet length (cm) | 10.5 | 10.5 | 10.5 | 10.5 | 7 |
| Beam pipe diameter (cm) | 3.6 | 3.6 | 3.6 | 3.6 | 3.6 |

In the transport line, an array of up to fourteen scanners is used to monitor the beam profiles over the whole line. Each scanner consists of a 32 micron diameter carbon filament for the measurement of the dense beam core and a pair of 1.5mm thick plate scraper for the measurement of the low density halo region. The beam profile scanner can provide intensity measurements over a dynamic range of about $10^5$. The philosophy for scanner locations is the following: the first group of two scanners located after Quadrupole 5 and 6 are used to measure the X and Y beam distribution at the exit of the RFQ respectively and provide a critical initial condition on the halo evolution. As we know, for the matched beam, the beams evolve and form an envelope oscillation with a same period as the LATTICE, but the RMS mismatched beams evolve and form a long period envelope oscillation in a linear focusing beam transport line. Although the oscillation

*Work supported by NSFC (91126003) and State Key Development Program of Basic Research of China (2007CB209904)
#ouyanghf@ihep.ac.cn



ISBN 978-3-95450-118-2

amplitude depends on the mismatch strength, the period is only related to the focusing strength but not the mismatch strength. For example, with the zero current phase advance of about 90° per period, about 6 envelope oscillations will develop along the transport line for the mismatched beams. For the present LATTICE, with the maximum gradient of the quadrupole magnets setting, up to 150° phase advance per period could be got. To observe halo formation, the other two groups of scanners with 6 scanners for each group are placed after Quadrupole 17 to 28, covering completely three full envelope oscillations for the mismatched beams. Scanners of the first and the second group are used to monitor the beam profile in X direction and Y direction alternately. Scanners of the third group are all used to monitor the beam profiles in X direction.

## BEAM PARAMETERS GOT AT THE EXIT OF RFQ

As mentioned in the last section, the two wire scanners in the first group, which locate after the quadrupole 5 and the quadrupole 6, are used to measure the beam profiles in X direction and Y direction, respectively. As a critical initial condition on the halo evolution, they are useful for the upcoming halo experiments and multi-particle tracking simulation.

As known, the beam ellipse transformation from position 1 to 2 can be expressed in matrix form as [1]

$$\sigma_2 = R\sigma_1 R^T \tag{1}$$

Where $R$ is transfer matrix between the two positions and $R^T$ is the transpose of matrix R. The beam ellipse matrix $\sigma$ is defined as

$$\sigma = \begin{pmatrix} \beta\varepsilon & -\alpha\varepsilon \\ -\alpha\varepsilon & \gamma\varepsilon \end{pmatrix}. \tag{2}$$

*where* $\alpha$, $\beta$ *and* $\gamma$ are the Twiss parameters and $\varepsilon$ is the un-normalized emittance. From Eq. (1) and Eq. (2), one can get

$$\beta_2\varepsilon_2 = R_{11}^2\beta_1\varepsilon_1 - 2R_{11}R_{12}\alpha_1\varepsilon_1 + R_{12}^2\gamma_1\varepsilon_1 \tag{3}$$

Let $\alpha_1$, $\beta_1$, $\gamma_1$, $\varepsilon_1$ denote the initial beam ellipse parameters at the exit of RFQ, and $\alpha_2$, $\beta_2$, $\gamma_2$, $\varepsilon_2$ denote the beam ellipse parameters at the beam profile measurement location. Since the Twiss parameters satisfy the relationship of $\beta\gamma-\alpha^2 = 1$ and the measured RMS beam size $X_{RMS}$ is equal to $\sqrt{\beta_2\varepsilon_{2,RMS}}$, Eq. (3) can be expressed as

$$X_{RMS}^2 = R_{11}^2 a + 2R_{11}R_{12}b + R_{12}^2 c \tag{4}$$

where $a = \beta_1\varepsilon_1$, $b = -\alpha_1\varepsilon_1$, $c = (1+\alpha_1^2)/\beta_1\varepsilon_1$. To obtain the measured RMS beam size $X_{RMS}$, Gaussian fitting is performed for the measured beam profile data at the wire scanner. In principle, on basis of Eq. (4), the transverse phase space ellipse parameters of beam at exit of RFQ can be calculated with three measured beam profiles got at three different quadrupole field settings. However, in the experiments, because of the existence of different errors, the equation set with only three equations usually has no solution or the solutions differ between each other. To avoid these problems, the equation set with more than three independent linear equations is generally taken use and in the meantime the least square method is also applied.

To determine the beam ellipse parameters at the exit of the RFQ, the simulation code TRACE-3D is used to compute the transfer matrices and to track the beams from the exit of RFQ to the measurement location. Since TRACE-3D deals the space charge forces with linearity, and in the meantime, the transfer matrices depend on the beam current and the beam profiles, the iterative method is taken in the calculations. The zero current and the simulated emittance at the exit of RFQ are used as the initial beam set for TRACE-3D in the first iteration. The successive iterations then use the solutions got in the last iteration as the input beam parameters of TRACE-3D. In order to get the solutions efficiently and correctly, a code is written to solve the equation set，to edit TRACE-3D input file, to call TRACE-3D and read the transfer matrix elements automatically. In Table2, the got beam parameter at the exit of RFQ is shown. There is about 50% difference between the simulated emittance and the calculated one both in X and Y direction.

Table 2: Beam Parameters at the Exit of RFQ

| $\alpha_x$ | $\beta_x$ (mm/mrad) | $\alpha_y$ | $\beta_y$ (mm/mrad) | $\varepsilon_x$ (π.mm.mrad) | $\varepsilon_y$ (π.mm.mrad) |
|---|---|---|---|---|---|
| 3.129 | 0.385 | -0.546 | 0.112 | 19.869 | 18.931 |

## COMPARISON BETWEEN SIMULATION AND EXPERIMENT

The output beam from RFQ is used in the experiments. The beam current is about 20mA. To avoid beam destruction to the thin wires used for measurement of the beam profiles, the beam is pulsed at the repetition rate of 1Hz and the pulse length of 50 microseconds. In simulation, the initial distribution is generated from the simulation of RFQ. The transverse phase-space plot of the distribution is given in Fig. 2. As shown in Fig. 2, the halo in the initial RFQ distribution already exists. With this initial distribution at an input beam current of 20mA, simulations are carried out for the beam transportation through the 28-quadrupole beam transport line with PARMILA code. In general, 50000 macro-particles per bunch are used in simulations. Space charge interaction is calculated via the 2-dimensional particle in cell (PIC) method with a 40×40 mesh and the mesh size is 0.05cm. In the simulations, the parameters of the 28 quadrupoles adopted are completely the same as those in the experiments.



ISBN 978-3-95450-118-2

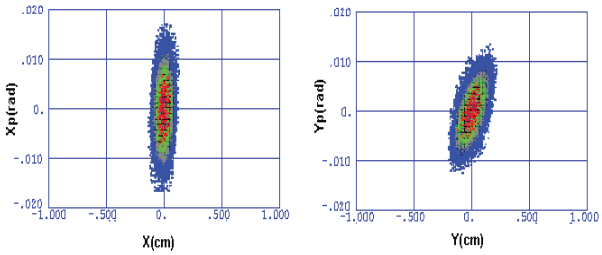


Figure 2: The transverse phase-space projections of the initial distribution.

In experiments, the first four quadrupoles were adjusted to produce match. The matching quadrupole gradients are obtained by producing equal rms beam size at different locations and the rms beam sizes are calculated from the measured beam profiles. The density profiles of the matched beam from simulations and from measurements are compared and shown in Fig. 3. As shown in the figure, in the middle of the beam transport line, the simulated beam profile is smaller than the measured one. At the end of the beam transport line, the simulated profile agrees well with the measured one. The results show that, in the matched case, the profiles from the simulated distribution are in good agreement with the shape of measured profiles. The result got above provides a good guidance for the beam pipe design of linac that runs at about 20mA beam current.

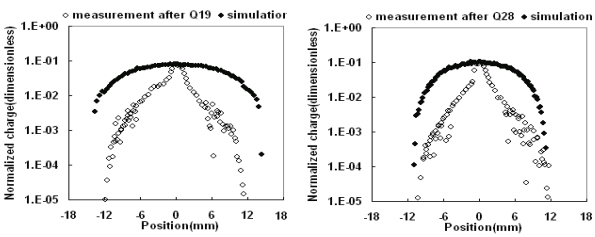


Figure 4: The horizontal profiles from measurements (circles) and simulations (dots) at the 5# (left) and 14# (right) wire scanner for 20mA mismatched beam.

The first four quadrupoles are also adjusted to produce mismatch. The comparison of the mismatched beam profiles between the simulated and the measured ones is shown in Fig. 5. As shown in the two figures, the simulation predicts well the maximum beam size, however, unlike the matched case, it fails to reform the shape of the measured profile. For the simulated beams, the particle density differences between the core and the tail are in an order of $10^3$. The simulated beams tend to form a uniform core with short extent edge rather than halo. For the measured beam, the particle density differences between the core and the tail are in an order of $10^4$. The measured profile shows broader shoulders and asymmetric features, which are the prominent features of halo in the mismatched beams [5]. Also, we checked the beam profiles after each quadruple along the beam line for simulated mismatched beams and couldn't find these features. It illustrates that no halo forms in the simulated

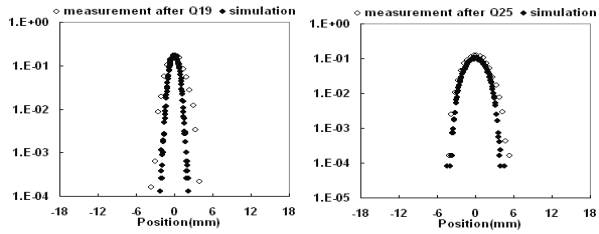


Figure 3: The horizontal profiles from measurement (circles) and simulation (dots) at the 5# (left) and 11# (right) wire scanners for 20mA matched beam.

beams. After that, we investigated the effects of mesh sizes and used 3D PIC code to calculate nonlinear space charge force. But the results have no significant change. To approach the measured beam, we added the manufacturing errors of magnets in simulations and found that the simulated beam profiles with errors are nearly the same as those without errors except a small quantity of beam center shift.

## CONCLUSIONS

With the beam halo experiment transport line, the main beam parameters at the exit of a RFQ are determined by experiments. Then comparison between the multi-particle simulations of 20mA beam and the measurement data is carried out. The initial distribution used is from multi-particle simulations of RFQ. The maximum amplitudes of the measured beam are consistent with the predictions from numerical simulations. The simulated profiles of matched beam are in good agreement with the measurement. However, the computer simulations failed to reproduce the shape of the measured mismatched profiles. The measured mismatched beam profiles exhibit prominent shoulders, which aren't observed in the simulated beams. The effects of mesh sizes, calculation methods of space charge force and magnet errors are studied with no significant change in results. Since the maximum number of particles and the mesh number of 3D space charge calculation of PARMILA code are constrained in small range, we need to do more simulations with other multi-particles codes.

## REFERENCES

[1] M. Reiser *Theory and Design of Charged Particle Beams*. John Wiley & Sons, New York, 1994.
[2] T.P. Wangler et al., Phys. Rev. ST Accel. Beams, 084201 (1998) 1.
[3] J. Qiang et al., Phys. Rev. ST Accel. Beams, 124201 (2002) 5.
[4] P.L. Colestock et al., "The Beam Halo Experiment at LEDA", Linac2000, Monterey, California, p806 (2000).
[5] T.P. Wangler et al., "Experimental Study of Proton-beam Halo Induced by Beam Mismatch in LEDA", PAC2001, Chicago, p2923 (2001).



ISBN 978-3-95450-118-2